Minor Changes in the Macrocyclic Ligands but Major Consequences on the Efficiency of Gold Nanoparticles Designed for Radiosensitization

*Gautier Laurent,[a] Claire Bernhard,[b] Sandrine Dufort,[c] Gloria Jiménez Sánchez,[a] Rana Bazzi,[a] Frédéric Boschetti,[d] Mathieu Moreau,[b] Trong-Hung Vu,[b] Bertrand Collin,[b,e] Alexandra Oudot,[e] Nirmitha Herath,[f] Herwig Requardt,[g] Sophie Laurent,[h] Luce Vander Elst,[h] Robert Muller,[h] Marie Dutreix,[f] Michel Meyer,[b] François Brunotte,[e] Pascal Perriat,[i] François Lux,[j] Olivier Tillement,[j] Géraldine Le Duc,[g] Franck Denat,[b] Stéphane Roux[a]**

[a] Institut UTINAM, UMR 6213 CNRS-UBFC, Université de Bourgogne Franche-Comté, 25030 Besançon Cedex, France. [b] Institut de Chimie Moléculaire de l'Université de Bourgogne (ICMUB), UMR 6302 CNRS-UBFC, Université de Bourgogne Franche-Comté, 21078 Dijon Cedex, France. [c] Nano-H S.A.S, 2 Place de l'Europe, 38070 Saint Quentin-Fallavier, France. [d] CheMatech S.A.S., 21000 Dijon, France. [e] Plateforme d'imagerie préclinique, Centre Georges-François Leclerc, 21079 Dijon Cedex, France. [f] Recombinaison, réparation et cancer : de la molécule au patient, Institut Curie, UMR CNRS 3347 - Inserm U1021, 91405 Orsay, France. [g] ID17 Biomedical Beamline, European Synchrotron Radiation Facility, 38000 Grenoble, France. [h] NMR Laboratory, Université de Mons, 7000 Mons, Belgium. [i] Matériaux Ingénierie et Science, UMR 5510 CNRS−INSA, INSA de Lyon, 69621 Villeurbanne Cedex, France. [j] Institut Lumière Matière, UMR 5306 CNRS-UCBL, Université Claude Bernard Lyon 1, 69622 Villeurbanne Cedex, France.

Ligand purification and analysis. All analyses were performed at the "Plateforme d'Analyses Chimiques et de Synthèse Moléculaire de l'Université de Bourgogne". The ^{1}H and ^{13}C NMR spectra were recorded at 300 or 330 K on 300, 500, or 600 MHz spectrometers (Bruker) using perdeuterated solvents. All chemical shifts were referenced to the protio peak. Mass spectra were obtained in the MALDI/TOF reflectron mode on an Ultraflex II LRF 2000 (Bruker) spectrometer using dithranol as a matrix or by ESI on an AmaZon SL spectrometer (Bruker). Elemental analyses were performed with a Flash EA 1112 CHNS instrument from Thermo. HPLC analyses were performed by using a Submit (Dionex) apparatus (C18 column Acclaim 120®, 3 μm, 150 × 4.6 mm) equipped with an UV detector (λ = 201, 214, 220, and 254 nm).

Chemicals and Reagents. All chemicals and solvents were used without further purification. DO_3A^tBu-(*N*-2-aminoethylethanamide) and DOTAGA-NH_2 were obtained from CheMatech® and used without further purification.

Synthesis of DTDOTA (3)

2-Bromoethyl(trityl)sulfane (1). 420 mg of ethylene sulfide (7 mmol) were added to a solution of triphenylmethylbromide (1.1 g, 3.5 mmol) in dichloromethane (10 mL). The mixture was stirred overnight at room temperature. The solvent was evaporated to dryness to remove the excess of ethylene sulfide and the resulting white solid was dissolved in dichloromethane (5 mL). Ethanol was added (15 mL) and the solution was left standing for 1 h to complete crystallization of **1**. The precipitate was filtered, washed with ethanol, and dried under vacuum to give pure **1** as colorless crystals (1.1 g, yield = 85%). ^{1}H NMR (300 MHz, $CDCl_3$, 300 K) δ (ppm): 2.71–2.94 (m, 4H), 7.20–7.51 (m, 15H). $^{13}C\{^{1}H\}$ NMR (75 MHz,

$CDCl_3$, 300 K) δ (ppm): 30.0 (CH_2), 34.2 (CH_2), 67.4 (CS), 126.2 (Ar, 3C), 128.1 (Ar, 6C), 129.5 (Ar, 6C), 144.5 (Ar, 3C). MALDI-TOF: *m/z* = 406.99 $[M+Na]^+$.

DO_3A^tBu-DT (2). 9.68 g of **1** (25 mmol, 4 equiv.) were added to a solution of DO_3A^tBu-(*N*-2-aminoethylethanamide) (3.88 g, 6.3 mmol), K_2CO_3 (5.23 g, 38 mmol), and sodium iodide (3.75 g, 25 mmol, 4 equiv.) in 1,4-dioxane (120 mL). The resulting mixture was heated at 60 °C overnight. After cooling, the solution was filtered on Celite, and the solvent was evaporated. Acetonitrile (200 mL) was added, the impurities were eliminated by filtration and the solvent was evaporated. The residue was purified by chromatography on aluminum oxide (eluent: CH_2Cl_2/MeOH 99.5:0.5) to give compound DO_3A^tBu-DT (**2**) as a yellow oil (2.3 g, yield = 30%). ^1H NMR (300 MHz, $CDCl_3$, 300 K) δ (ppm): 1.37 (s, 18H, $OC(CH_3)_3$), 1.39 (s, 9H, $OC(CH_3)_3$), 2.04–3.44 (m, 36H), 6.91 (b s, 1H), 7.10–7.24 (m, 20H), 7.25–7.37 (m, 10H). ESI-MS: *m/z* = 977.55 $[M–Trityl+H]^+$, 1219.65 $[M+H]^+$, 1241.63 $[M+Na]^+$.

DTDOTA (3). 1.1 g (0.90 mmol) of compound **2** were dissolved in 15 mL of a 20% HCl solution. The mixture was stirred for 12 h at 50 °C. Water (5 mL) was added and the resulting solution was washed with dichloromethane and lyophilized to give DTDOTA•3HCl (**3**•3HCl) as a yellow solid (360 mg, yield = 64%). ^1H NMR (300 MHz, D_2O, 300 K) δ (ppm): 2.91 (t, 2H, ^3J = 7.2 Hz), 3.04–4.06 (m, 34H). ESI-MS: *m/z* = 567.26 $[M+H]^+$, 589.25 $[M+Na]^+$, 1129.49 $[(M–2H)+H]^+$, 1151.47 $[(M–2H)+Na]^+$.

Synthesis of TADOTA (7) and TADOTAGA (8)

TA-NHS (4). 10.79 g of disuccimidyl carbonate, 98% (42 mmol, 1.5 equiv.), 11.7 mL of NEt_3 (84 mmol, 3 equiv.) were added to a solution of thioctic acid (5.8 g, 28 mmol) in CH_3CN (300 mL). The resulting mixture was stirred at room temperature for 4 h. After evaporation of the solvent, the residue was dissolved in 100 mL of ethyl acetate, washed with 2 x 100 mL of a 5% sodium bicarbonate solution. The organic phase was extracted and dried over $MgSO_4$.

Evaporation of the solvent afforded TA-NHS (**4**) as a yellow solid (8.46 g, yield = 99%). ^{1}H NMR (300 MHz, $CDCl_3$, 300 K) δ (ppm): 1.19–1.32 (m, 1H), 1.35–1.80 (m, 9H), 1.82–1.94 (m, 1H), 2.39–2.49 (m, 1H), 2.52–2.66 (m, 2H), 3.01–3.19 (m, 2H), 3.48–3.60 (m, 1H). ^{13}C{^{1}H} NMR (75 MHz, $CDCl_3$, 300 K) δ (ppm): 24.3, 25.7 (2C), 28.4, 30.8, 34.5, 38.6, 40.3, 56.7, 168.4, 169.3 (2C).

TADOTA (7). 10 g (16 mmol) of DO_3A^tBu-(*N*-2-aminoethylethanamide) were dissolved in 32 mL of HCl 37%. The mixture was stirred at room temperature for 20 min before evaporating the solvent. Acetone was added and the white precipitate was isolated by filtration to give the salt DOTA-NH_2•3HCl•3H_2O (9.63 g, 16 mmol, yield = 100%). The salt of DOTA-NH_2 and *N*,*N*-diisopropylethylamine (11.3 mL) were dissolved in a mixture of water/CH_3CN (1:1) until pH = 9 was reached. TA-NHS (**4**) (7.22 g, 24 mmol, 1.5 equiv.) was added and the mixture was stirred overnight at room temperature. After evaporation of the solvent, the residue was dissolved in 40 mL of water and the impurities were eliminated by filtration. The solution was acidified until pH = 2 with 37% HCl. The product was deprotonated on Amberlite® IRA-458 ion-exchange resin (eluent: CH_3COOH 5%), affording TA-DOTA (**7**) as a white solid (10.1 g, yield = 98%) with a 98% HPLC purity (eluent: A: CH_3CN / B: H_2O + 0.4% HCOOH, B 98% to 0%; rt = 6.98 min). ^{1}H NMR (300 MHz, D_2O, 300 K) δ (ppm): 1.27–1.53 (m, 3H), 1.55, 1.86 (m, 4H), 1.97–2.10 (m, 1H), 2.28–2.35 (m, 2H), 2.47–2.60 (m, 1H), 2.96–3.66 (m, 25H), 3.68–3.79 (m, 1H), 3.80–3.96 (m, 4H). ^{13}C{^{1}H} NMR (75 MHz, D_2O, 330 K) δ (ppm): 25.3, 28.2, 34.0, 36.0, 38.6, 38.8, 39.1, 40.6, 48.6 (2C), 48.8 (2C), 51.3 (2C), 52.0 (*C*H_2, 2C), 54.3 (CH), 56.2, 57.0 (2C), 57.1 (CH_2), 169.9 (2C), 172.2, 175.1, 177.4 (C=O). ESI-MS: *m/z* = 635.33 $[M+H]^+$, 663.45 $[M–H]^–$. Elemental analysis for $C_{26}H_{46}N_6O_8S_2$•4H_2O: calculated: C (44.18%), N (11.89%), H (7.70%); obtained: C (43.97%), N (11.60%), H (7.98%).

TA-DOTAGA (8). 13.6 g (15 mmol) of DOTAGA-NH_2 and 21.4 mL (123 mmol, 8 equiv.) of *N*,*N*-diisopropylethylamine were dissolved in 154 mL of water, the solution reaching pH 9 at equilibrium. CH_3CN was added to obtain a 1:1 mixture of H_2O/CH_3CN. 9.4 g (31 mmol, 2 equiv.) of TA-NHS (**6**) were added and the mixture was stirred overnight at room temperature. After evaporation of the solvent, the residue was dissolved in 40 mL of water and the impurities were eliminated by filtration. The solution was acidified until pH = 2 with 37% HCl. The product was deprotonated on Amberlite® IRA-458 ion-exchange resin (eluent: CH_3COOH 5%), affording TA-DOTAGA (**8**) as a white solid (11.7 g, yield = 97 %) with a 98% HPLC purity (eluent: A: CH_3CN / B: H_2O + 0.4% HCOOH, 98% to 0%; rt = 7.65 min). ^1H NMR (300 MHz, D_2O, 300 K) δ (ppm): 1.31–1.48 (m, 3H), 1.55–1.81 (m, 4H), 1.84–2.10 (m, 3H), 2.18–2.32 (m, 2H), 2.37–2.60 (m, 3H), 2.90–4.01 (m, 29H). ESI-MS: *m/z* = 707.32 $[M+H]^+$, 705.45 $[M–H]^–$. Elemental analysis for $C_{29}H_{50}N_6O_{10}S_2•4H_2O$: calculated: C (44.72%), N (10.79%), H (7.51%); obtained: C (44.61%), N (10.62%), H (8.05%).

UV–visible spectroscopy. UV–visible absorption spectra of functionalized gold nanoparticle colloidal suspensions were recorded at room temperature with a SPECORD 250 spectrophotometer (Analytic Jena AG) in the 400–800 nm range. The spectral measurements were performed on a diluted colloid introduced in a standard quartz cuvette.

Hydrodynamic diameter and zeta potential measurements. Direct determination of the hydrodynamic diameter and zeta potential of nanoparticles was performed with a Zetasizer from Malvern Instrument. The suspension was diluted to obtain a concentration of 0.08 $g.L^{-1}$ in an aqueous solution (for hydrodynamic diameter measurements) and in NaCl (0.01 M) aqueous solution adjusted to the desired pH.

Transmission electron microscopy (TEM). TEM was used to obtain detailed morphological information about the samples and was carried out using a JEOL 2010 microscope operating

at 200 kV. The samples for TEM were prepared by depositing a drop of a diluted colloidal solution (Au@DTDOTA, Au@TADOTA, and Au@TADOTAGA) on a carbon grid and allowing the liquid to dry in air at room temperature.

Thermogravimetric analyses (TGA). TGA were performed with a DISCOVERY device (TA Instruments), on ca. 2 mg of freeze-dried samples, under an air flow and a heating rate of 5 °C.min^{-1} in the temperature range 25–700 °C.

Acid–base potentiometric titrations. Au@TADOTA nanoparticles (V_{assay} = 0.8 mL, [Au] = 10 g/L in water) suspended in 25 mL of a 0.1 M KNO_3 supporting electrolyte solution was acidified to pH ca. 3 by 0.1 M HCl and then titrated up to pH 11.6 by standardized 0.1 M KOH under an argon atmosphere and controlled temperature (T = 298.2(2) K). The experimental setup, conditions, and data treatment were identical to those previously described in detail elsewhere.[1] The thermodynamic reversibility was checked by cycling from low to high pH and vice versa. The colloidal suspension evidenced no coagulation over the entire pH range, but irreversible titration curves were obtained above pH 8, as a result of chemical degradation. While the inflection points enabled to determine the total amount of titrated ligand, the degradation prevented a reliable estimation of the protonation constants of the TADOTA moiety anchored to the gold surface, as at least two of them are expected to be above 10^9.

NMR spectroscopy. Proton Nuclear Magnetic Relaxation Dispersion (NMRD) profiles extending from 0.25 mT to 0.94 T (0.01 – 40 MHz) were recorded with a Fast Field Cycling Relaxometer (Stelar, Mede, Italy) on 0.6 mL solutions contained in 10-mm o.d. tubes at 37°C.

Proton relaxation times (T_1 and T_2) were also measured at 0.47 T and 1.41 T with Minispec mq-20 and mq-60 (Bruker, Karlsruhe, Germany) at 37°C. The samples were composed of

gadolinium chelates coated gold nanoparticles ([Au] = 45 mM and 1.7 mM ≤ [Gd] ≤ 7.5 mM) dispersed in aqueous solution at pH 7.4

Radiolabeling of gold nanoparticles by ^{111}In and purification. The preparation of ^{111}In-labelled Au@TADOTA-Gd and Au@TADOTAGA-Gd nanoparticles was simply realized by mixing the gold nanoparticles in buffered saline solution (pH~7.4) with an $^{111}InCl_3$ solution in diluted hydrochloric acid. Briefly, 150 MBq of high purity $^{111}InCl_3$ was added to 1 mL of gold nanoparticles (~50 mM Au). The mixture was incubated for 30 min at room temperature. The radiolabeled nanoparticles were separated from $^{111}InCl_3$ on a PD-10 column (GE Healthcare Bio-Sciences AB, Uppsala, Sweden) as follows. The PD-10 column was first equilibrated with 15 mL of 50 mM citrate buffer (pH = 5). The radiolabelling solution was then loaded on the PD-10 column, and fractions of 0.5 mL were eluted with 50 mM citrate buffer (pH = 5). Radiolabeled Au@TADOTA-Gd and Au@TADOTAGA-Gd nanoparticles were first eluted as a light brown suspension. The radioactivity of each fraction was counted using an ionization chamber (Capintec Radioisotope Calibrator CRC-15, Capintec Inc., Ramsey, USA). Finally, the four fractions with the highest radioactivity were pooled. Radiochemical purity was determined by instant thin-layer chromatography (ITLC). ITLC of the purified nanoparticles was performed using silica gel plates (Gelman Science Inc., Ann Arbor, MI, USA), 50 mM citrate buffer (pH = 5) as the eluent, and a TLC scanner (MiniGita, Raytest, Isotopenmessgeräte, GmbH, Straubenhardt, Germany) in order to determine the percentage of free $^{111}InCl_3$. Radiolabeled gold nanoparticles remained at the origin (Rf = 0), whereas residual $^{111}InCl_3$ migrated with an Rf of 0.8.

Post-mortem **ICP-MS analyses.** Collected organs were dehydrated in drying oven before to be mineralized in hot ultrapure *aqua regia* in high purity polypropylene tubes (DigiTUBEs, SCP Science, Courtaboeuf, France). Before mineralization, each hemisphere of the brain was

separated. The gold content in collected organs was determined by ICP-MS using a 7500ce spectrometer (Agilent Technologies, Les Ulis, France).

Radiation source and MRT setup. Microbeam Radiation Therapy (MRT) was performed at the ID17 biomedical beamline at the European Synchrotron Radiation Facility (Grenoble, France). MRT uses X-rays emitted tangentially to the ring from relativistic electron bunches circulating in a storage ring. The wiggler source produces a white spectrum of photons that extends after filtration (Be (0.5mm), C (1.5mm), Al (1.5mm), and Cu (1.0 mm)) from 50 to 350 keV (mean energy of 90 keV). The quasilaminar beam is spatially fractionated into an array of microbeams by using an adjustable multislit collimator positioned 41.7 m from the photon source and 100 cm upstream from the head of the animals. Upstream from the multislit collimator, the dose rate within a homogeneous field of 10 mm × 10 mm was approximately 90 $Gy.s^{-1}.mA^{-1}$. Downstream of the multislit collimator, the peak entrance dose within the microbeam was ~72 $Gy.s^{-1}.mA^{-1}$.

RESULTS AND DISCUSSION

During the first hour after intravenous injection, we observed that urine is colored in brown. This suggests that a large part of nanoparticles were quickly removed by urine. This was confirmed by ICP (inductively coupled plasma) analyses and TEM (transmission electron microscopy) experiments (Fig. S1). TEM experiments performed with urine after intravenous injection of Au@TADOTAGA-Gd nanoparticles showed that nanoparticles are present in urine and the size of the gold core remains the same. The presence of the nanoparticles in the urine and the preservation of the size are the signs of an absence of ligand desorption. The partial desorption of the organic shell should indeed favor the agglomeration of the nanoparticles. As a consequence, the partial desorption should be accompanied by a limited

renal clearance. This is not the case for Au@TADOTAGA-Gd and Au@TADOTA-Gd nanoparticles. The SPECT signal in bladder is therefore due to the presence of radiolabeled nanoparticles.

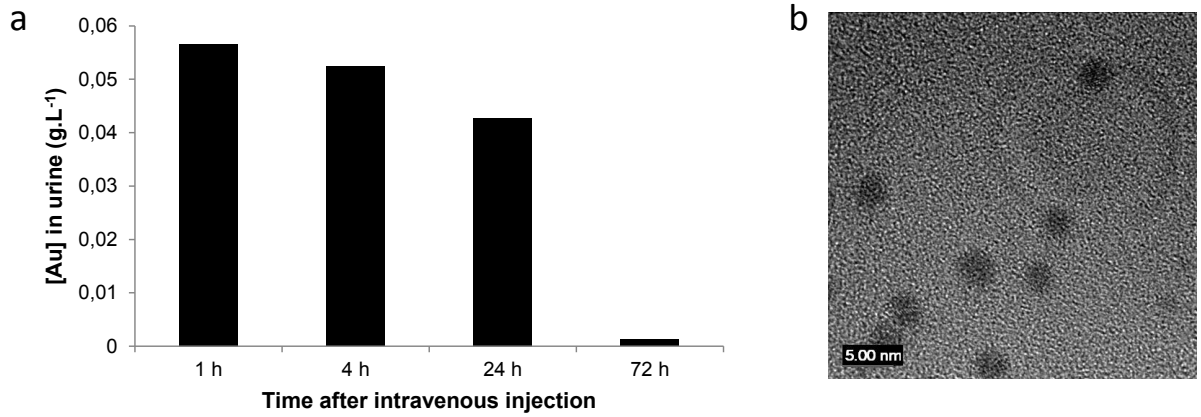

Fig. S1. *Renal clearance of Au@TADOTAGA-Gd nanoparticles. (a) gold concentration in urine determined by ICP at different time points. (b) TEM micrograph of gold nanoparticles present in the urine after intravenous injection of the gold nanoparticles.*

REFERENCE

(1) Meyer, M.; Frémond, L.; Tabard, A.; Espinosa, E.; Vollmer, G. Y.; Guilard, R.; Dory, Y. Synthesis, Characterization and X-ray Crystal Structures of Cyclam Derivatives. Part VI. Proton Binding Studies of a Pyridine-Strapped 5,12-Dioxocyclam Based Macrobicycle. *New J. Chem.* **2005**, *29*, 99–108.